

## Origin of Oxygen Induced Layer-By-Layer Growth in Homoepitaxy on Pt(111)

Stefanie Esch, Michael Hohage, Thomas Michely, and George Comsa

*Institut für Grenzflächenforschung und Vakuumphysik, Forschungszentrum Jülich, D-52425 Jülich, Germany*

(Received 16 July 1993; revised manuscript received 8 November 1993)

Whereas on the clean Pt(111) surface Pt grows in a multilayer (3D) mode at 300 and 400 K, preadsorption of an ordered  $p(2\times 2)$  oxygen overlayer leads to a high quality layer-by-layer (2D) growth with the oxygen floating on the film. In contrast to other surfactants oxygen can be completely removed from the film surface at the growth temperature. It is demonstrated that the presence of oxygen reduces the barrier height for the motion of Pt adatoms across step edges. This facilitates the interlayer mass transport and thus the layer-by-layer growth.

PACS numbers: 68.55.Jk, 61.16.Ch, 68.55.Ce, 68.55.Ln

Recently surfactants have attracted considerable interest in both hetero- and homoepitaxial growth by increasing the smoothness of the deposited films [1-4]. However, so far the technological application of surfactants to the growth of smooth films is hampered by the difficulty of removing the floating adsorbed overlayer from the deposited film after growth process completion. In fact, surfactants like As and Sb which successfully alter the growth of films to layer-by-layer growth are almost unremovable even at elevated temperatures [2-4]. From this point of view the use of simple gases, which can often be removed more easily, would be desirable [1]. This is especially true for the growth of heterosystems where temperature treatments would cause interdiffusion. For homoepitaxial growth on Pt(111) it was noticed by He scattering that oxygen supplied from the background gas during growth improves the Pt interlayer mass transport, the *sine qua non* condition for 2D growth [5].

In this Letter we will demonstrate that an oxygen overlayer is very effective in inducing a greatly reduced film roughness during homoepitaxy on Pt(111). Moreover, the oxygen overlayer is floating on the film and can be completely removed by hydrogen exposure at room temperature, leaving a clean and smooth film behind.

In view of the fact that films are usually grown far from equilibrium (high supersaturation), the mechanisms by which the additives change the growth mode have to be found in modifications of the growth kinetics. Two mechanisms have been proposed so far to be effective in changing the growth mode in the case of homoepitaxy: (1) the increase of the island number density [6] and (2) the lowering of the barrier for adatoms at step edges which hinders the interlayer diffusion [4]. Both mechanisms can in principle play an important role. Whereas the effectiveness of the first one has been demonstrated experimentally [6], the present scanning tunneling microscope (STM) study gives the first direct experimental evidence of the second one, that an additive can lower the barrier at step edges.

The STM, the UHV apparatus, and the sample preparation are described in detail elsewhere [7,8]. Here, Pt was grown on the Pt(111) surface precovered with an oxygen overlayer and for comparison on the same but

clean Pt(111) surface at identical surface temperature and deposition rate. The oxygen precovered sample is prepared by exposing it to a pressure of  $p_{\text{oxygen}} \approx 2 \times 10^{-5}$  mbar for 5 min starting from 500 K while cooling from the last annealing. The oxygen is adsorbed atomically at fcc threefold hollow sites [9] and forms an ordered  $p(2\times 2)$  overlayer leading to a sharp low energy electron diffraction pattern. Throughout the range of applied voltages ( $\pm 600$  mV) and currents ( $\leq 15$  nA) oxygen is imaged as a depression on the surface. The pattern of dark spots in hexagonal arrangement in Fig. 1 is thus the  $p(2\times 2)$ O superstructure. The adlayer is not perfect but shows some apparent oxygen vacancies. It was necessary to replace oxygen on the surface after about 2-3 grown layers since oxygen was partly reacted away by residual  $\text{H}_2$  and CO during Pt deposition, as the corresponding partial pressures are rising due to the heating up of the evaporator surroundings.

The Pt vapor phase deposition is done by sublimating an ultrapure Pt foil heated by electron bombardment. If not otherwise specified the deposition rate is  $4.4 \times 10^{-3}$  monolayer (ML) per second. Two deposition temperatures (300 and 400 K) were chosen. They lie in the range where the growth of *clean* Pt(111) proceeds in the 3D mode. After processing the Pt(111) surface at a temperature  $T$ , no thermal annealing is observed when continu-

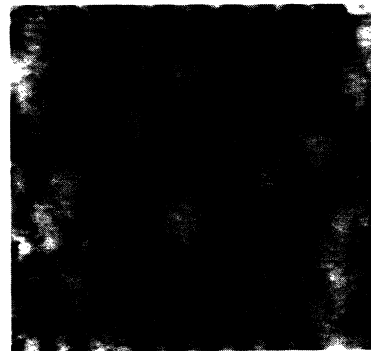


FIG. 1. The  $p(2\times 2)$ O overlayer on Pt(111) recorded at 200 K. The arrangement of dark spots corresponds to the positions of adsorbed oxygen atoms ( $60 \text{ \AA} \times 60 \text{ \AA}$ ).

ing to keep the sample at this temperature, if  $T \leq 400$  K [8]. Thus the STM topographs obtained at room temperature represent the true morphology at the end of the deposition.

The influence of oxygen on the growth behavior is obvious in Fig. 2 when comparing the STM topographs obtained after the deposition of approximately 5 ML of Pt on the clean and the oxygen precovered surfaces. In the clean case the deposited Pt forms pyramidal structures with up to 8 and 10 uncovered layers at 300 K [Fig. 2(a)] and 400 K [Fig. 2(c)], respectively. In contrast, on the oxygen precovered surface only 5 layers are uncovered at both temperatures [Figs. 2(b) and 2(d)]. The morphology of the film grown on the oxygen precovered surface is obviously much smoother.

For a more quantitative comparison the fractions of uncovered layers were determined by means of image analysis [10] in a number of topographs like those in Figs. 2(a)–2(d). The degree of completion of the depos-

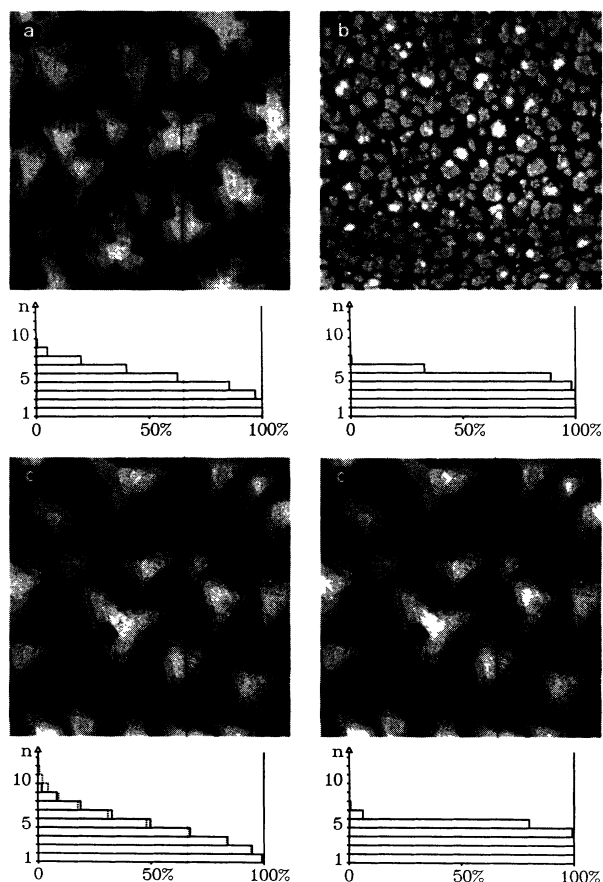


FIG. 2. Topographs taken after deposition of approximately 5 ML of Pt on the clean surface at 300 K (a) and 400 K (c) and on the oxygen precovered surface at 300 K (b) and 400 K (d) [ $1100 \text{ \AA} \times 1100 \text{ \AA}$  in (a) and (b);  $2200 \text{ \AA} \times 2200 \text{ \AA}$  in (c) and (d)]. The percentage of completion of the deposited layers versus the layer number  $n$  is plotted as a histogram below each topograph.

ited layers is shown as a histogram below the corresponding STM images in Fig. 2.

The difference in growth behavior between the clean and the oxygen preadsorbed cases appears to be most pronounced at 400 K. The growth is close to the ideal 3D and 2D behavior, respectively. Indeed, the histogram in Fig. 2(c) deviates only slightly from a Poisson distribution, shown dashed in the same plot. (The Poisson distribution corresponds to the ideal 3D growth [11].) In contrast, in Fig. 2(d) only a few Pt atoms in layers 6 and 7 are in the "wrong layer"; i.e., almost all Pt atoms falling on growing islands have managed to join the lower levels.

Figure 3 shows a detail of a STM image after the deposition of 5 ML of Pt on the oxygen precovered surface. Besides areas vacant of oxygen (i.e., where oxygen has been lost to the gas phase leaving the clean surface behind) there are still patches of the  $p(2 \times 2)\text{O}$  overlayer floating on the terrace and oxygen atoms decorating the step edges of the islands. An exact determination of the oxygen coverage during growth is not possible. After reacting away the oxygen with gas-phase  $\text{H}_2$  at room temperature, no oxygen could be detected with Auger spectroscopy, demonstrating that no appreciable amount has been incorporated into the film.

The experiments and discussion so far have shown that in the presence of preadsorbed oxygen the interlayer mass transport (i.e., the jumping of adatoms across step edges onto the lower terrace) is dramatically increased.

An enhancement of this interlayer mass transport can be caused by either increasing the attempt frequency of the deposited atoms to overcome the potential barrier at the island rim for descending on the lower terrace [6], or by lowering this potential barrier [4]. The effect of increasing the attempt frequency was demonstrated recent-

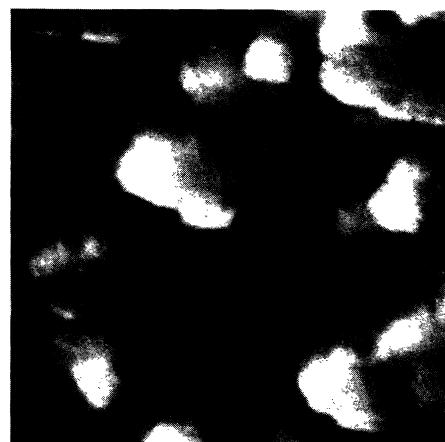


FIG. 3. Topograph taken after the deposition of approximately 5 ML of Pt on the oxygen precovered surface at 300 K [see Fig. 2(b)]. The topograph is represented with illumination from the left. Oxygen is floating on the terrace [patches of the  $p(2 \times 2)\text{O}$  adlayer] and is decorating the step edges of the islands ( $140 \text{ \AA} \times 140 \text{ \AA}$ ).

ly in the case of Ag/Ag(111) [6]. The island number density was artificially increased and thus the maximal size of the islands before coalescence set in was decreased, however, without decreasing the mobility of the Ag adatoms on top of the islands. The ensuing layer-by-layer growth showed that decreasing the island size while keeping the diffusivity on top of the islands high results in an increased interlayer mass transport. We will call this the size effect [12].

Figure 4 shows that the Pt island number density on the oxygen precovered Pt(111) surface [Fig. 4(b)] is increased by a factor of 16 compared to the clean case [Fig. 4(a)], due to the reduced diffusivity of the Pt adatoms on the oxygen covered terraces. At first sight one might thus ascribe the smoothing effect of oxygen demonstrated in Fig. 2 to this increase of the island number density, i.e., to the size effect. This explanation could be used here if no oxygen were to be present on top of the islands. If, however, the islands were oxygen covered to the same extent as the terraces, the diffusivity of the Pt adatoms on top of the islands would also be reduced to the same extent as on the terraces and nucleation before coalescence should be expected. Figure 3 shows that some oxygen is, indeed, present on the islands 30 min after the end of the growth (and thus even more during the growth process)—even if we cannot ascertain that in the same amount as on the terrace. We conclude that the effect of oxygen on the growth mode via the size effect is certainly less important than the density increase may suggest.

In order to assess the possible contribution to the growth mode change demonstrated in Fig. 2 to an oxygen induced reduction of the barrier at the edge of the islands, we performed a number of experiments. The result of one of them is shown in Fig. 5. In this experiment we directly determined the fraction of the Pt adatoms which

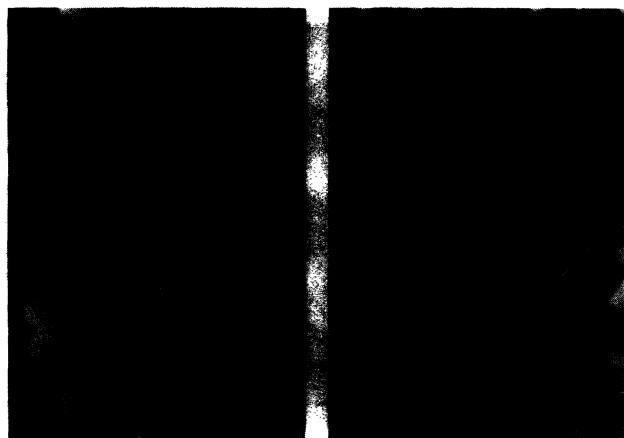


FIG. 4. Topographs taken after deposition of 0.2 ML of Pt at 400 K (a) on the clean Pt(111) surface and (b) on the oxygen covered surface. The topographs are represented with illumination from the left [ $2200 \text{ \AA} \times 1450 \text{ \AA}$ ; inset in (b):  $550 \text{ \AA} \times 360 \text{ \AA}$ ].

remained on top of preexistent islands out of those which landed on them (and thus the magnitude of the interlayer mass transport) for the “clean” and the “oxygen covered” cases, while largely excluding the size effect. The experiment consisted of a preparation step and a subsequent growth step. In the preparation step we deposited  $X$  ML of Pt at 400 K with a rate of  $3.3 \times 10^{-3}$  ML/s. A 60 s annealing at 620 K led to islands of rather homogeneous size and shape [Figs. 5(a) and 5(b)]. Note that no second layer islands are present on the top of the islands. In the subsequent growth step we deposited *identical* amounts of  $Y$  ML of Pt at the *same* rate and temperature ( $3.4 \times 10^{-4}$  ML/s, 350 K) onto the prepared islands in two different runs: (1) after covering the prepared islands with oxygen [the “oxygen” run, Fig. 5(c)] and (2) on freshly prepared islands [the “clean” run, Fig. 5(d)]. The amounts  $Y = 6.5 \times 10^{-2}$  ML deposited during 193 s in both runs and leading to the morphology in Figs. 5(c) and 5(d) have been verified *a posteriori* from the analysis of many STM images to be identical for the two runs within the experimental error margin of  $\pm 0.4 \times 10^{-2}$  ML. The remarkable homogeneity of the island sizes in Fig. 5(d) (we refer here to the first layer islands present on the terrace) shows that due to the choice of deposition parameters hardly any new islands have been nucleated on the terrace during the clean growth; except for the few very small islands which we will disregard, all others (which we will call *C* islands) originate from the further growth of the islands nucleated during the preparation stage. In contrast, in Fig. 5(c) obtained after the oxygen

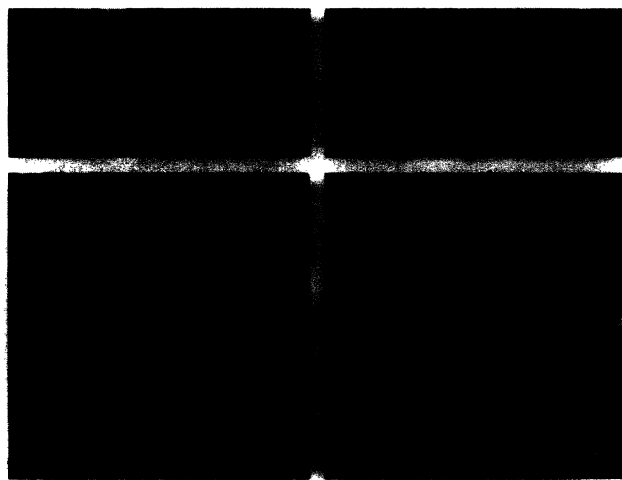


FIG. 5. Topographs (a) and (b) taken at the end of the preparation step, i.e., after deposition of  $11.7 \times 10^{-2}$  ML and  $7.8 \times 10^{-2}$  ML of Pt, respectively, at 400 K and subsequent annealing to 620 K. Topographs (c) and (d) taken at the end of the growth step, i.e., after the deposition of  $6.5 \times 10^{-2}$  ML of Pt at 350 K (c) on the surface shown in (a) but oxygen covered, and (d) on the surface shown in (b) left as prepared (see text) [ $1100 \text{ \AA} \times 2200 \text{ \AA}$  in (a) and (b);  $2200 \text{ \AA} \times 2200 \text{ \AA}$  in (c) and (d)].

growth, two categories of islands are present on the terrace, small and large ones, each one rather homogeneously sized. The small ones have obviously been nucleated during the oxygen growth. Their high density is due to the reduced Pt adatom diffusivity on the terrace caused by the presence of oxygen (see Fig. 4 and the corresponding text). The large ones—on which we will focus in the following—originate, like the *C* islands, from the further growth of the prepared ones, but now in the presence of oxygen; we call them *O* islands.

The amounts  $X_O$  and  $X_C$  deposited in the preparation steps of the oxygen and of the clean growth, respectively, were chosen so that the final sizes of the *O* and *C* islands became approximately equal. Because the *O* islands are growing more slowly at equal deposition rates (nearly half of the Pt atoms landing on the oxygen covered terrace are “consumed” in the nucleation and growth of the small islands), we had to take  $X_O > X_C$ . The particular values in the experiments shown in Figs. 5(a) and 5(b) have been  $X_O = (11.7 \pm 0.3) \times 10^{-2}$  ML and  $X_C = (7.8 \times 0.3) \times 10^{-2}$  ML. They ensured that during the *whole* growth step the *O* islands were larger than the *C* ones and thus that the island size effect (discussed above) alone would clearly favor Pt nucleation on top of the *O* islands during the growth step.

A simple comparison between Figs. 5(c) and 5(d) shows that the contrary is the case: The nucleation probability on top of the *C* islands is much larger than on the *O* ones *and* the size of each of the islands nucleated on top of the *C* islands is also much larger. This, in spite of the fact that all conceivable processes clearly favored Pt nucleation and accumulation on top of the *O* islands: (a) the size effect (see above), (b) the reduced diffusivity of the Pt adatoms due to the adsorbed oxygen on top of the *O* islands, and (c) the larger number of Pt atoms which landed on each of the *O* islands due to their larger size during the growth step (identical Pt exposures). In order to be more quantitative we determined for both the *C* and the *O* islands the number of Pt atoms which have landed on them during the growth step (assuming that the island area increases linearly in time) and of those which were present on top of the islands at the end of this step [from images like those in Fig. 5(c) and 5(d)]. From these numbers we deduce that the fraction of the Pt atoms which jumped onto the lower terrace after having landed

onto the *C* and *O* islands are  $(22.4 \pm 4.4)\%$  and  $(90.0 \pm 1.3)\%$ , respectively; and this in spite of the processes listed above, which tend to ease the jumping down from the *C* islands compared to the *O* ones.

The only plausible explanation for this unequivocal result is that the adsorbed oxygen reduces substantially the barrier at the step edges which hinders the interlayer mass transport for the clean Pt/Pt(111) system. This effect alone is sufficient to explain the oxygen induced layer-by-layer growth in homoepitaxy on Pt(111), which does not exclude an additional contribution of the size effect.

The authors acknowledge helpful discussions with Bene Poelsema, Georg Rosenfeld, Laurens Verheij, and Michael Bott.

- 
- [1] W. F. Egelhoff and D. A. Steigerwald, *J. Vac. Sci. Technol. A* **7**, 2167 (1989).
  - [2] M. Copel, M. C. Reuter, E. Kaxiras, and R. M. Tromp, *Phys. Rev. Lett.* **63**, 632 (1989).
  - [3] M. Horn-Von Hoegen, F. K. LeGoues, M. Copel, M. C. Reuter, and R. M. Tromp, *Phys. Rev. Lett.* **67**, 1130 (1991); N. Grandjean, J. Massies, and V. H. Etgens, *Phys. Rev. Lett.* **69**, 796 (1992).
  - [4] H. A. van der Vegt, H. M. van Pinxteren, M. Lohmeier, E. Vlieg, and J. M. C. Thornton, *Phys. Rev. Lett.* **68**, 3335 (1992).
  - [5] B. Poelsema, R. Kunkel, N. Nagel, A. F. Becker, G. Rosenfeld, L. K. Verheij, and G. Comsa, *Appl. Phys. A* **53**, 369 (1991).
  - [6] G. Rosenfeld, R. Servaty, C. Teichert, B. Poelsema, and G. Comsa, *Phys. Rev. Lett.* **71**, 895 (1993).
  - [7] K. Besocke, *Surf. Sci.* **181**, 145 (1987).
  - [8] T. Michely, Ph. D. thesis, Jül-Bericht 2569, Jülich, 1991.
  - [9] K. Mortensen, C. Klink, F. Jensen, F. Besenbacher, and I. Stensgaard, *Surf. Sci.* **220**, L701 (1989).
  - [10] Image analysis program by ProScope, An Kuckum 30, D-52146 Würselen.
  - [11] B. Poelsema and G. Comsa, *Scattering of Thermal Energy Atoms* (Springer, Berlin, 1989).
  - [12] In addition to the increased attempt frequency, a contribution to the size effect also originates in the increase of the time interval between the successive arrivals of deposited atoms on an island due to its smaller size. The increase of these time intervals tends to render nucleation more difficult.

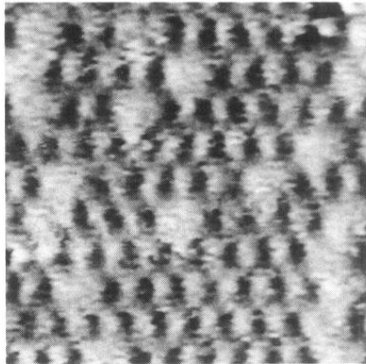


FIG. 1. The  $p(2\times 2)\text{O}$  overlayer on Pt(111) recorded at 200 K. The arrangement of dark spots corresponds to the positions of adsorbed oxygen atoms ( $60 \text{ \AA} \times 60 \text{ \AA}$ ).

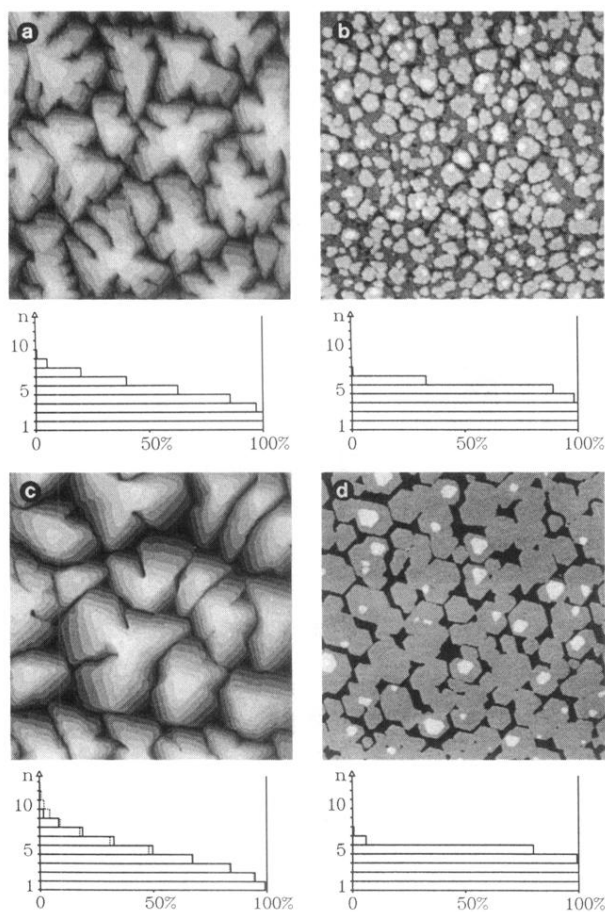


FIG. 2. Topographs taken after deposition of approximately 5 ML of Pt on the clean surface at 300 K (a) and 400 K (c) and on the oxygen precovered surface at 300 K (b) and 400 K (d) [ $1100 \text{ \AA} \times 1100 \text{ \AA}$  in (a) and (b);  $2200 \text{ \AA} \times 2200 \text{ \AA}$  in (c) and (d)]. The percentage of completion of the deposited layers versus the layer number  $n$  is plotted as a histogram below each topograph.

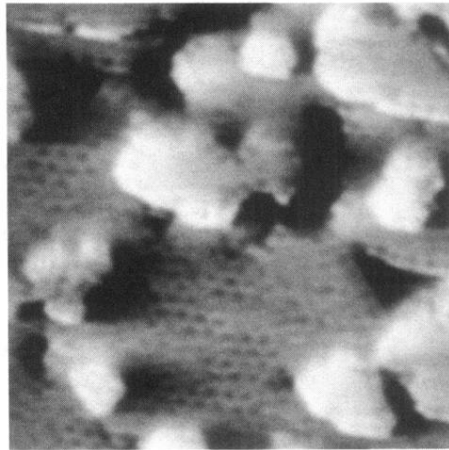


FIG. 3. Topograph taken after the deposition of approximately 5 ML of Pt on the oxygen precovered surface at 300 K [see Fig. 2(b)]. The topograph is represented with illumination from the left. Oxygen is floating on the terrace [patches of the  $p(2 \times 2)O$  adlayer] and is decorating the step edges of the islands ( $140 \text{ \AA} \times 140 \text{ \AA}$ ).

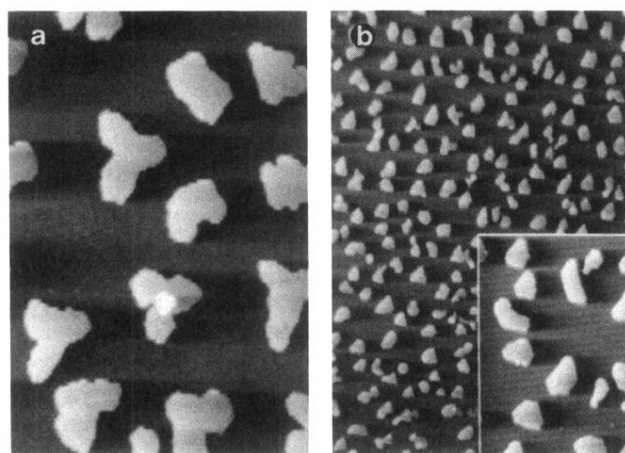


FIG. 4. Topographs taken after deposition of 0.2 ML of Pt at 400 K (a) on the clean Pt(111) surface and (b) on the oxygen covered surface. The topographs are represented with illumination from the left [ $2200 \text{ \AA} \times 1450 \text{ \AA}$ ; inset in (b):  $550 \text{ \AA} \times 360 \text{ \AA}$ ].

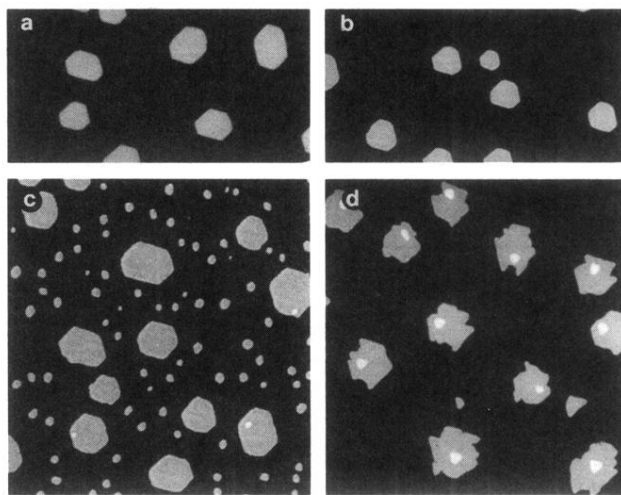


FIG. 5. Topographs (a) and (b) taken at the end of the preparation step, i.e., after deposition of  $11.7 \times 10^{-2}$  ML and  $7.8 \times 10^{-2}$  ML of Pt, respectively, at 400 K and subsequent annealing to 620 K. Topographs (c) and (d) taken at the end of the growth step, i.e., after the deposition of  $6.5 \times 10^{-2}$  ML of Pt at 350 K (c) on the surface shown in (a) but oxygen covered, and (d) on the surface shown in (b) left as prepared (see text) [ $1100 \text{ \AA} \times 2200 \text{ \AA}$  in (a) and (b);  $2200 \text{ \AA} \times 2200 \text{ \AA}$  in (c) and (d)].